

# Direct-Coupled Cavity Filters for Wide and Narrow Bandwidths\*

LEO YOUNG†, SENIOR MEMBER, IEEE

**Summary**—Direct-coupled resonator filters in transmission line are discussed. The resonators consist of sections of transmission line coupled either by series capacitances or shunt inductances. Over narrow frequency bands, such filters show characteristics similar to those of lumped-constant filters and their design is straightforward. The design of direct-coupled resonator filters over wide (as well as narrow) frequency bands is presented here using the quarter-wave transformer as a prototype circuit. Several numerical examples (with fractional bandwidths between 10 per cent and 85 per cent) are worked out to illustrate the method. It is shown that the response can be improved by optimizing the line impedances.

## I. INTRODUCTION

THE BAND-PASS FILTER design techniques discussed in this paper are based on the quarter-wave transformer prototype circuit [1], [2]. They apply to band-pass filters with transmission-line resonators alternating between coupling elements which are series capacitances or shunt inductances. The design bandwidths may range from narrow-band on up to such wide bandwidths that the filters can be used for microwave high-pass applications. The two types of filter considered here are shown schematically in Figs. 1 and 2. The design of other types of band-pass filters over wide bandwidths has been treated by Matthaei [3]. The design of direct-coupled resonator filters, as shown in Figs. 1 and 2, but with only narrow or moderate bandwidths, has been treated by Cohn [4], Riblet [5] and others. The design viewpoint of this paper was developed to obtain a design method which would hold for wider bandwidths and for smaller pass-band Chebyshev ripples as well.

Section II introduces the quarter-wave transformer prototype circuit, and Section III gives basic design formulas for synchronously tuned filters.

Section IV treats narrow-band filters from the present viewpoint, showing the connection with the lumped-constant low-pass prototype [4]. It has been found that the design technique of Section IV for narrow-band filters generally works well up to fractional bandwidths of about 20 per cent or more, provided that the pass-band ripple is not too small; the ripple VSWR should exceed about  $1 + (2w)^2$ , where  $w$  is the fractional bandwidth of the narrow-band filter, if it is to be derivable from a lumped-constant low-pass prototype.

The remainder of this paper, from Section V on, is

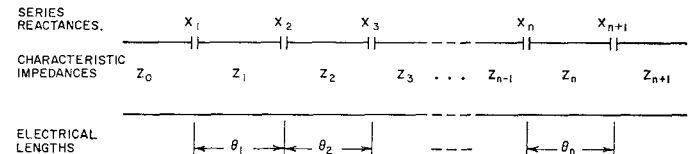


Fig. 1—Reactance-coupled half-wave filter with series-capacitance couplings.

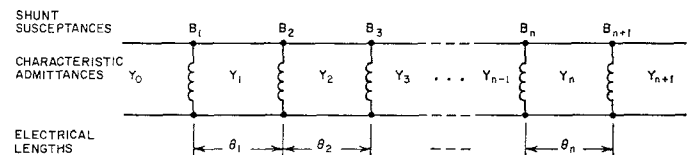


Fig. 2—Reactance-coupled half-wave filter with shunt-inductance couplings.

concerned mainly with the design of wide-band and pseudo-high-pass filters, for which the method of the quarter-wave transformer prototype is principally intended. The basic theory, design data, and examples will be found in Sections V through VIII.

In this paper the frequency will be introduced everywhere as the normalized frequency, usually denoted by  $f/f_0$ , the ratio of the frequency  $f$  to the synchronous frequency  $f_0$ . For waveguide filters the "normalized frequency" is to be understood to refer to the quantity  $\lambda_{g0}/\lambda_g$ , the ratio of the guide wavelength  $\lambda_{g0}$  at the frequency of synchronous tuning, to the guide wavelength  $\lambda_g$ .

## II. FILTERS WITH IMPEDANCE STEPS AND IMPEDANCE INVERTERS

Stepped-impedance filters (quarter-wave transformers and half-wave filters) have been treated by Young [1]. This section points out their equivalence to filters with impedance inverters, and serves as an introduction to the design of wide-band reactance-coupled half-wave filters.

An impedance (or admittance) step [Fig. 3(a)] can always be replaced by an impedance (or admittance) inverter [Fig. 3(b) and (c)] without affecting the filter response curve, provided that the input and output ports are properly terminated. Thus the two types of circuit in Fig. 3 are entirely equivalent as a starting point for the design of filters. The impedance-inverter (or admittance-inverter) point of view [Fig. 3(b) and (c)] is the more natural one to adopt to convert the lumped-constant low-pass prototype into a transmis-

\* Received November 23, 1962. This work was sponsored by the U. S. Army Signal Research and Development Laboratory, Fort Monmouth, N. J., under Contract DA 36-039 SC-87398.

† Stanford Research Institute, Menlo Park, Calif.

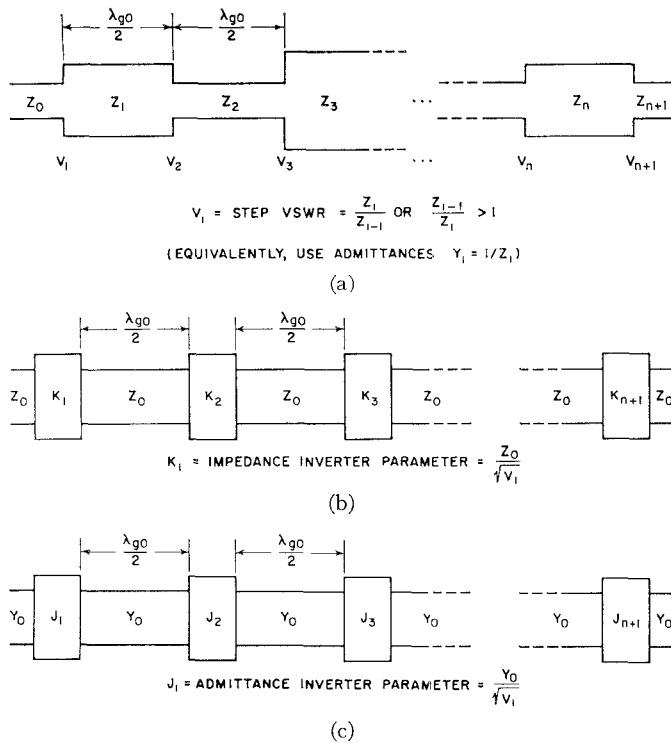


Fig. 3—A stepped-impedance half-wave filter and equivalent filters using impedance or admittance inverters. (a) Half-wave filter with stepped impedances. (b) Half-wave filter with ideal impedance inverters. (c) Half-wave filter with ideal admittance inverters.

sion-line filter [4]; whereas a stepped-impedance-filter point of view is more convenient to utilize directly the design data of Young [1].

The stepped-impedance filter is turned into a reactance-coupled filter by replacing each impedance step with a reactance having the same discontinuity VSWR [1] and spacing the reactances to obtain synchronous tuning (Section III).

One important difference in approach between this paper and earlier work [4] is that in this paper the starting point or prototype circuit is one of the circuits in Fig. 3 (the synthesis of which is precisely controlled), whereas for narrow-band filters the exact synthesis may be pushed back one stage to the lumped-constant prototype circuit of Cohn [4]. For example, the performance of the circuits shown in Fig. 3(b) and (c), having ideal inverters, would not give exactly the prescribed response if designed by the methods of Cohn [4] (although the approximation would be very close for narrow or moderate bandwidths). However, the circuits in Fig. 3(b) and (c) have transmission characteristics identical to those of the half-wave filter in Fig. 3(a).

The frequency behavior of the reactive discontinuities (shunt-inductances or series-capacitances) is examined in detail. The behavior of the discontinuities leads to increasing distortion of the filter response (e.g., pass-band bandwidth and stop-band attenuation), as the frequency spread is increased. This type of consideration can be left out in the design of narrow-band filters, thereby simplifying the design process considerably.

However, it is important to predict the distortion for filters having large bandwidths.

A quarter-wave transformer and the notation associated with it is shown in Fig. 4. The characteristics of maximally flat and Chebyshev quarter-wave transformers are sketched in Fig. 5. Closely related to the quarter-wave transformer is the stepped-impedance half-wave filter [1] sketched in Fig. 6. Its characteristics, shown in Fig. 7, are similar to those of the quarter-wave transformer shown in Fig. 5. If the impedance steps or junction VSWR's  $V_i$  ( $i=1, 2, \dots, n+1$ ) of a quarter-wave transformer and a stepped-impedance half-wave filter are the same, then the characteristics of the latter can be obtained from those of the former by a linear change of scale on the frequency axis; the stepped-impedance half-wave filter bandwidth becomes one half the quarter-wave transformer bandwidth.

The parameter  $R$  is again defined [1] as the product of the discontinuity VSWR's.

$$R = V_1 V_2 \cdots V_{n+1}. \quad (1)$$

If the fractional bandwidth  $w$  is less than about 20 per cent, and if [1]

$$R \gg \left(\frac{1}{w}\right)^n, \quad (2)$$

then the filter may be considered narrow-band; this case will be treated in Section IV.

The quarter-wave transformer prototype circuit is suitable for designing reactance-coupled filters up to very large bandwidths. As a result it is subject to certain limitations that do not complicate narrow-band design procedures. It is well to understand these differences at the outset. Basically they arise from the fact that it is not possible to convert the specified performance of the filter into the performance of the appropriate prototype transformer over large frequency bands by means of simple equations or tabulated functions. Instead, the frequency variations of the reactive couplings have been used to modify the known response functions of quarter-wave transformers to predict the performance of the derived filters (Figs. 1 and 2) over large frequency ranges. Thus it is possible from the graphs to quickly calculate the principal filter characteristics from the transformer characteristics, but not the other way round, as would be more desirable. In the case of wide-band designs where the variation of reactive coupling across the pass band is appreciable, it is necessary first to guess what prototype should be used, and then to match the predicted filter performance against the specified filter performance; if they are not close enough, the process must be repeated with another prototype. What makes this method feasible and practical is the speed with which, by means of the design graphs, this prediction can be made. Most of these design graphs will be presented in Section V.

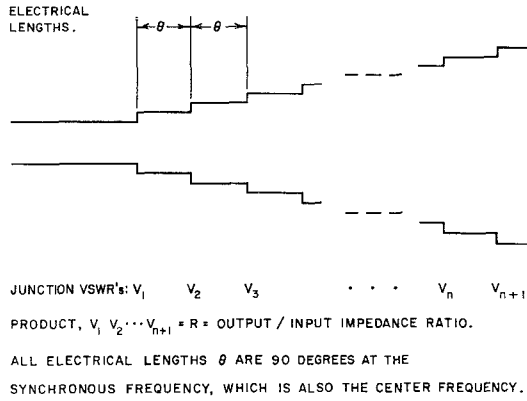


Fig. 4—Quarter-wave transformer used in prototype circuit.

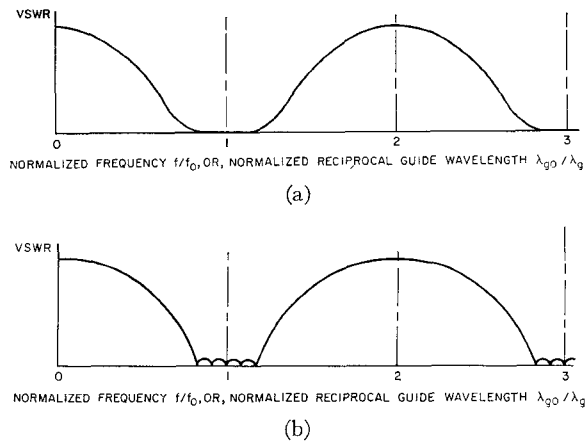


Fig. 5—Quarter-wave transformer characteristics. (a) Maximally flat. (b) Chebyshev.

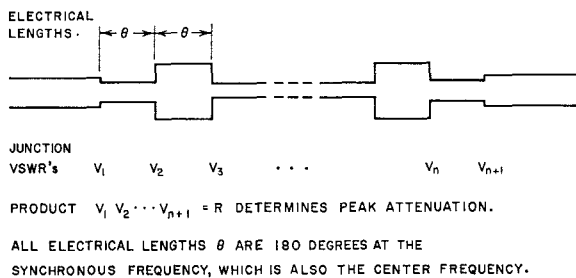


Fig. 6—Stepped half-wave filter used as prototype circuit.

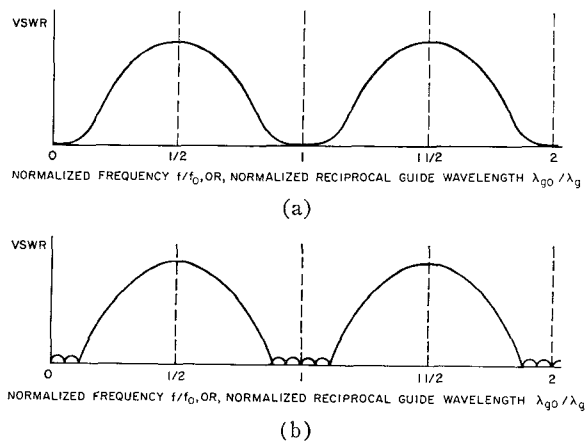


Fig. 7—Stepped half-wave filter characteristics. (a) Maximally flat. (b) Chebyshev.

### III. SYNCHRONOUSLY TUNED REACTANCE-COUPLED HALF-WAVE FILTERS

Band-pass filters of the two configurations shown in Figs. 1 and 2 are of considerable practical importance since they are easily realized in practice. These two circuits are duals of each other. The first, shown in Fig. 1, consists of a number of series capacitances alternating with a number of transmission-line sections; the second, shown in Fig. 2, consists of a number of shunt inductances alternating with a number of transmission-line sections. Both filters will be called reactance-coupled *half-wave* filters, in the sense that all line lengths between reactances approach one-half wavelength (or a multiple thereof) as the couplings become weak. Each line length between discontinuities constitutes a resonator, so that the filters in Figs. 1 and 2 have  $n$  resonators. Notice that the series elements in Fig. 1 are stipulated to be capacitances, that is, their susceptances are supposed to be positive and proportional to frequency. Similarly, the shunt elements in Fig. 2 are stipulated to be inductances, that is, their reactances are supposed to be positive and proportional to frequency. (If the transmission line is dispersive, these statements are to be modified by replacing frequency by reciprocal guide wavelength.)

All the filters described in this paper are synchronously tuned [1], that is, all discontinuities are so spaced that the reflections from any two adjacent discontinuities are phased to give maximum cancellation at a fixed frequency (the synchronous frequency) in the pass band. At the synchronous frequency the filter is interchangeable with a stepped-impedance half-wave filter [1], and the  $i$ th reactive discontinuity has the same discontinuity VSWR,  $V_i$ , as the  $i$ th impedance step [1], [2]. Impedances are shown for the series-reactance-coupled filter in Fig. 1 and admittances for the shunt-susceptance-coupled filter in Fig. 2; then, let

$$h_i = \frac{Z_i}{Z_{i-1}} \quad \text{or} \quad \frac{Y_i}{Y_{i-1}}, \quad (3)$$

and

$$u_i = \frac{X_i}{Z_{i-1}} \quad \text{or} \quad \frac{B_i}{Y_{i-1}}. \quad (4)$$

Most frequently  $h_i = 1$ , since usually this is mechanically the most convenient. Sometimes it may be advantageous for electrical or mechanical reasons to make some of the characteristic impedance ratios  $h_i$  different from unity. For instance, it may be desirable to combine the filter with an impedance transformer instead of cascading a filter with a separate transformer; also, in some cases the filter performance can be improved in the pass band when the values of  $h_i$  are selected carefully, as in Section VIII.

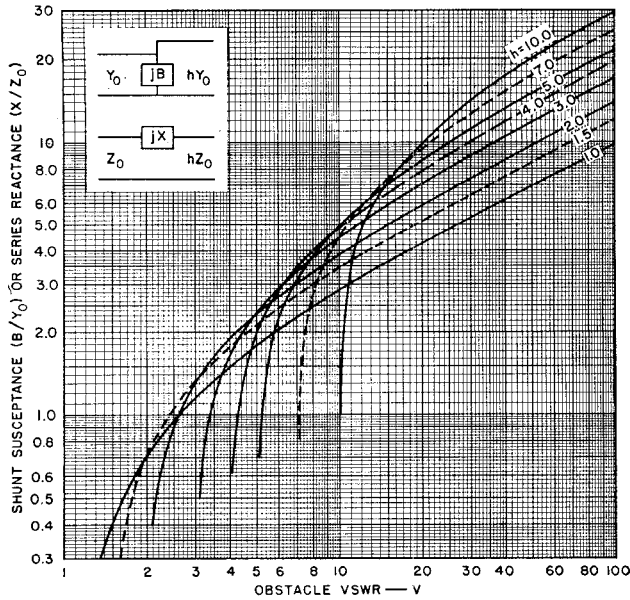


Fig. 8—Shunt susceptance (or series reactance) as a function of discontinuity VSWR for several characteristic admittance (or impedance) ratios,  $h$ .

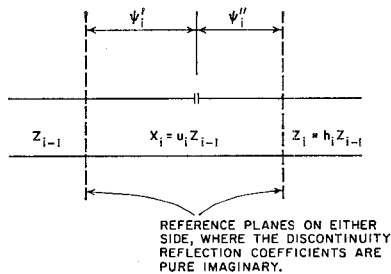


Fig. 9—Series-reactance coupling of two lines with different characteristic impedances.

The  $u_i$  of the reactance-coupled filter are obtained from the  $V_i$  of the stepped-impedance filter, and the  $h_i$ , from

$$u_i = \sqrt{\left(V_i + \frac{1}{V_i}\right) h_i - (1 + h_i^2)}. \quad (5)$$

The graph of Fig. 8 gives some solutions of this equation. Generally it will be most convenient to select  $h_i=1$  (that is, all the  $Z_i$  or  $Y_i$  equal), and then (5) simplifies to

$$u_i = \sqrt{V_i} - \frac{1}{\sqrt{V_i}}. \quad (6)$$

The spacings  $\theta_i$  in Fig. 1 are determined as follows [2], [6]. A single discontinuity of a series-reactance-coupled filter is shown in Fig. 9. (A similar notation, but with  $Y$  for  $Z$  and  $B$  for  $X$ , applies to a shunt-susceptance-coupled filter.) It represents the  $i$ th discontinuity of the filter (Fig. 1 or 2). If the reflection coefficients of this discontinuity in the two reference planes shown are to be pure imaginary quantities, then one has to set

$$\psi_i' = \frac{1}{2} \arctan \left( \frac{u_i^2 + h_i^2 - 1}{2u_i} \right) \quad (7)$$

$$\psi_i'' = \frac{1}{2} \arctan \left( \frac{u_i^2 + 1 - h_i^2}{2h_i u_i} \right). \quad (8)$$

The spacings  $\theta_i$  in Figs. 1 or 2 are now given (in radians) by

$$\theta_i = \frac{\pi}{2} + \psi_i'' + \psi_{i+1}'. \quad (9)$$

When  $h_i=1$ , these equations reduce to

$$\psi_i' = \psi_i'' = \psi_i = \frac{1}{2} \arctan \left( \frac{u_i}{2} \right), \quad (10)$$

and then

$$\begin{aligned} \theta_i &= \frac{\pi}{2} + \psi_i + \psi_{i+1} \\ &= \frac{\pi}{2} + \frac{1}{2} \left[ \arctan \left( \frac{u_i}{2} \right) + \arctan \left( \frac{u_{i+1}}{2} \right) \right] \\ &= \pi - \frac{1}{2} \left[ \arctan \left( \frac{2}{u_i} \right) + \arctan \left( \frac{2}{u_{i+1}} \right) \right] \end{aligned} \quad (11)$$

#### IV. NARROW-BAND HALF-WAVE FILTERS

The main application of this paper is to wide-band filters. However, since the design of narrow-band filters is simpler, it will be convenient to use the narrow-band case to illustrate the method in its simplest form.

When the impedance-steps of a narrow-band (Section I) stepped-impedance half-wave filter [1] are replaced by reactances having the same discontinuity VSWR's, and the filter is again synchronously tuned (Section III), then there is little change in the characteristics of the filter in and near the pass-band region. All the formulas necessary to carry out this conversion have been given in Section III. It is not necessary to maintain uniform line impedance (all  $Z_i$  or  $Y_i$  the same), but it is usually convenient to do so.

For narrow-band filters, both quarter-wave transformers and lumped-constant low-pass filters will serve as a prototype, and the conversion from either prototype into the actual filter is equally convenient. The choice of prototype depends on two factors:

- 1) Which prototype results in a filter that meets the design specifications more closely, and
- 2) Which prototype design is more readily available.

The quarter-wave transformer is better as regards point 1), but the difference in accuracy is usually negligible for narrow-band filters; the lumped-constant low-pass filter, on the other hand, is generally more convenient as regards point 2). The reason for this is that explicit formulas exist for the lumped-constant low-pass filter of  $n$  elements [4] whereas the numerical design of transformers demands great arithmetical accuracy, and

becomes convenient only for those cases where the solutions have been tabulated [1].

A lumped-constant low-pass filter can serve as a prototype circuit for a narrow-band stepped-impedance half-wave filter. Eqs. (74) of Young [1] with the substitution  $w_q = 2w$ , reduce to

$$V_1 = V_{n+1} = \frac{2}{\pi} \frac{g_1 \omega_1'}{w}$$

$$V_i = \frac{4}{\pi^2} \frac{\omega_1'^2}{w^2} g_{i-1} g_i, \dots, \text{ when } 2 \leq i \leq n, \quad (12)$$

where  $w$  is the fractional bandwidth of the narrow-band half-wave filter, and the  $g_i$  are the normalized elements of the low-pass prototype filter [4]. The reactances are then obtained from (5) or (6) and the spacings from (7)–(11). The low-pass prototype filter is here assumed to be either symmetric or antisymmetric, and element values for maximally flat and Chebyshev prototypes of this type can be found in Matthaei, *et al.* [7]. The parameter  $\omega_1'$  is the cutoff frequency of the low-pass prototype filter.

*Example:*<sup>1</sup> It is desired to design a reactance-coupled half-wave filter to have a pass-band VSWR of better than 1.10 over a 10 per cent bandwidth, and to have at least 25 db of attenuation at a frequency 10 per cent above band center (*i.e.*, twice as far out as the desired band edge).

This filter can be considered narrow-band, and may be based on a low-pass prototype circuit, since the ripple VSWR of 1.10 exceeds the quantity  $1 + (2w)^2 = 1.04$ , as mentioned in Section I.

We must next determine the minimum number of resonators with which these specifications can be met. Selecting a quarter-wave transformer of fractional bandwidth  $w_q = 0.20$ , since  $w = 0.10$ , and with  $V_r = 1.10$ , the attenuation at twice the band-edge frequency increment (see Example 7 of Young [1]) is 24.5 db for  $n = 5$  sections and 35.5 db for  $n = 6$  sections. Since the filter attenuation at the corresponding frequency above the pass band will be somewhat less than it was,  $n = 5$  is certainly not enough resonators. We then tentatively select  $n = 6$ . It will be shown in Section V that the attenuation in the stop band of the narrow-band reactance-coupled half-wave filters of Figs. 1 and 2 differ from the attenuation of the narrow-band stepped-impedance half-wave filter (Example 7, [1]) by approximately

$$\Delta L_A = 20(n + 1) \log_{10} (f_0/f) \text{ db}, \quad (13)$$

where  $f/f_0$  is the normalized frequency (the ratio of the frequency  $f$  to the center frequency  $f_0$ ). This  $\Delta L_A$  has to be added to the attenuation of the stepped-impedance filter to give the attenuation of the reactance-coupled filter.

<sup>1</sup> The filter example selected is the same as the one in Cohn's Fig. 9 [4], and Young's filter 1 [8], and corresponds to example 7 in Young [1], to make it more convenient to compare methods and properties.

Let us, for instance, calculate the attenuation of the filter at  $f/f_0 = 1.10$ . Using (13), with  $n = 6$ ,

$$\Delta L_A = -20 \times 7 \times \log_{10} (1.1) = -5.8 \text{ db}, \quad (14)$$

which shows that the filter attenuation is 5.8 db less than the attenuation of the half-wave stepped filter at  $f = 1.1 f_0$ , that is,  $35.5 - 5.8 = 29.7$  db. This exceeds the 25-db attenuation specified, which confirms our choice of  $n = 6$ . The discontinuity VSWR's are then given by (76) of [1]. The shunt-inductance-coupled filter of Fig. 2, with all  $Y_i$  equal to  $Y_0$ , yields

$$\left. \begin{aligned} \frac{B_1}{Y_0} = \frac{B_7}{Y_0} &= -1.780 \\ \frac{B_2}{Y_0} = \frac{B_6}{Y_0} &= -6.405 \\ \frac{B_3}{Y_0} = \frac{B_5}{Y_0} &= -9.544 \\ \frac{B_4}{Y_0} &= -10.154 \end{aligned} \right\}, \quad (15)$$

and from (11),

$$\left. \begin{aligned} \theta_1 = \theta_6 &= 147.16^\circ \\ \theta_2 = \theta_5 &= 165.41^\circ \\ \theta_3 = \theta_4 &= 168.51^\circ \end{aligned} \right\}. \quad (16)$$

This filter was analyzed and its computed response is shown in Fig. 10 (solid line) together with the computed response of the stepped-impedance half-wave filter (broken line). (The stepped-impedance half-wave filter has the same characteristics as the quarter-wave transformer, except for a linear change of scale, by a factor of 2, along the frequency axis.) It is seen that the band edges of the filter and its stepped-impedance half-wave filter prototype very nearly coincide, and that the peak ripples in the two pass bands are nearly the same height.

The VSWR ripple in the pass band is very close to 1.10. The quarter-wave transformer design is itself only approximate, and the ripple heights (broken line, top of Fig. 10) are not exactly the same, since the transformer was designed from a lumped-constant low-pass prototype (Example 7, [1]). The causes of imperfection in the filter response in Fig. 10 may in this case be ascribed partly to 1) the imperfect quarter-wave transformer response, since the transformer was derived by an approximation from a lumped-constant circuit, and partly to 2) the further approximation involved in deriving the filter with its unequal spacings and frequency-sensitive couplings from the transformer.

With regard to the imperfect quarter-wave transformer response, there is clearly little room for improvement, as can be seen from Fig. 10. As for the further approximations involved, one could adjust the line characteristic impedances to improve the performance (as is explained in Section VIII), but this would also

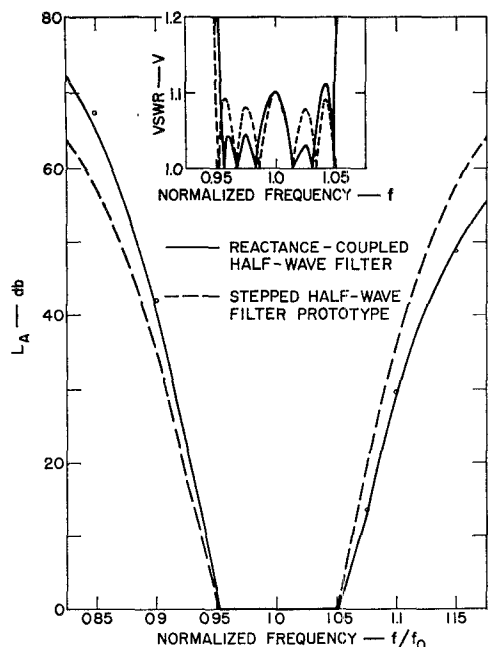


Fig. 10—Characteristics of a six-resonator filter and its stepped-impedance half-wave filter prototype.

result in only a very small improvement. These adjustments were not considered further in the present example.

The attenuation of the filter at  $f/f_0=1.1$  had been predicted from (13) to be 29.7 db. This gives one of the circle points in Fig. 10, and falls very close to the curve computed by analysis of the filter (solid line); other points predicted using (13) also fall very close to the computed curve.

#### V. DESIGN FOR SPECIFIED BAND EDGES AND STOP-BAND ATTENUATION

Typical characteristics of a quarter-wave transformer and the reactively coupled filter derived from it are shown in Fig. 11. The transformer prototype has a symmetrical response (broken line) on a frequency scale. Denoting its band edges by  $f_1'$  and  $f_2'$  (Fig. 11), the frequency of synchronous operation (Section III) is also the mean or center frequency,

$$f_0 = \frac{f_1' + f_2'}{2} \quad (17)$$

The response is symmetrical about  $f_0$ . When the impedance steps of the transformer are replaced by series capacitances or shunt inductances, then the new response is as indicated by the solid line in Fig. 11. The following general changes should be noted.

- 1) The bandwidth has contracted. (For small bandwidths this is the only change of major concern.)
- 2) The lower band edge has contracted ( $f_1'$  to  $f_1$ ) more than the upper band edge ( $f_2'$  to  $f_2$ ). If both the transformer and the filter have the same synchronous frequency  $f_0$ , then the new mean fre-

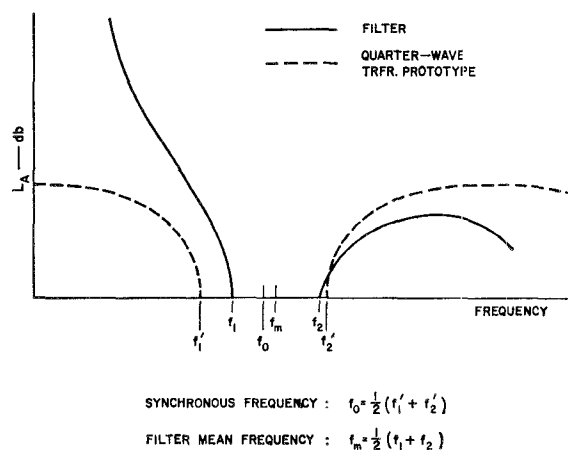


Fig. 11—General characteristics of reactance-coupled half-wave filter and quarter-wave transformer with same discontinuity VSWR's and same synchronous frequency.

quency (defined as the arithmetic mean of  $f_1$  and  $f_2$ )

$$f_m = \frac{f_1 + f_2}{2} \quad (18)$$

is greater than  $f_0$ , the frequency of synchronous tuning. Also, the two curves in the upper stop band cross each other, and the response is not symmetrical about  $f_m$ .

- 3) The ripple amplitude inside the pass band, for a Chebyshev filter, has not changed appreciably. (This is not indicated in Fig. 11.)

#### A. Bandwidth Contraction

We shall define the fractional bandwidth  $w$  of the filter in the usual way by

$$w = \frac{f_2 - f_1}{f_m} \quad (19)$$

The fractional bandwidth  $w_q$  of the transformer is

$$w_q = \frac{f_2' - f_1'}{f_0} \quad (20)$$

The bandwidth contraction factor  $\beta$  is then defined by

$$\beta = \frac{w}{w_q} \quad (21)$$

and can be obtained from the graphs given in Fig. 12 as a function of  $R$ , the ratio (greater than one) of the output impedance to the input impedance of the transformer prototype. For narrow bandwidths, the pass band is nearly symmetrical on a frequency scale, and so the bandwidth also determines the band edges. (For narrow-band filters,  $\beta$  will be close to 0.5, as in the example in Section IV.) For wide-band filters, the bandwidth contraction does not give the whole story, and one has to consider the movement of the two band edges separately, as will now be discussed.

B. Pass-Band Distortion

It will be shown in Section VII that one would expect the response to be approximately symmetrical when plotted not against frequency, but against the quantity

$$x = \frac{\Delta f}{(f/f_0)^\alpha} = \frac{f - f_0}{(f/f_0)^\alpha} \tag{22}$$

as shown in Fig. 13, and that for highly selective filters (filters corresponding to large transformer output-to-input impedance ratio  $R$ ), the exponent  $\alpha$  is given approximately by

$$\alpha \approx 1 + \frac{1}{n}, \tag{23}$$

where  $n$  is the number of transformer sections or filter

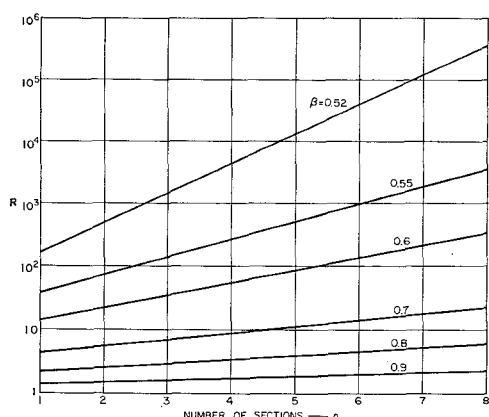


Fig. 12—Bandwidth contraction factor  $\beta$  as a function of  $n$  (number of resonators) and  $R$  (discontinuity-VSWR product.)

resonators. (The case  $\alpha \approx 1$ , corresponding to large  $n$ , leads to a symmetrical response on a wavelength scale, as previously noted by Cohn [4] using different arguments.)

When  $R$  approaches unity,  $\alpha$  will approach zero for synchronous filters for all  $n$ , regardless of the frequency dependence of the couplings. Thus any curve in Fig. 14 must pass through the origin. Similarly, (23) supplies the asymptotes for the graph of Fig. 14. Eq. (22) can be made exact for the two band-edge frequencies,  $f_1$  and  $f_2$ , by defining

$$\alpha = \frac{\log(\Delta f_2/\Delta f_1)}{\log(f_2/f_1)} \tag{24}$$

where

$$\left. \begin{aligned} \Delta f_2 &= f_2 - f_0 \\ \Delta f_1 &= f_0 - f_1 \end{aligned} \right\} \tag{25}$$

Eq. (24) will henceforth be used as the definition of  $\alpha$ .

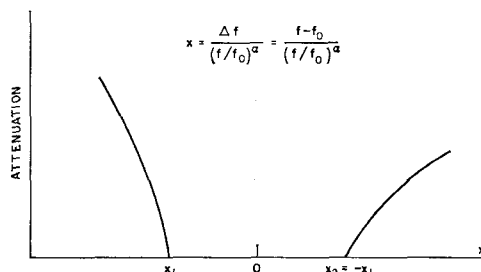


Fig. 13—A method of transforming the frequency variable to obtain an approximately symmetrical filter characteristic.

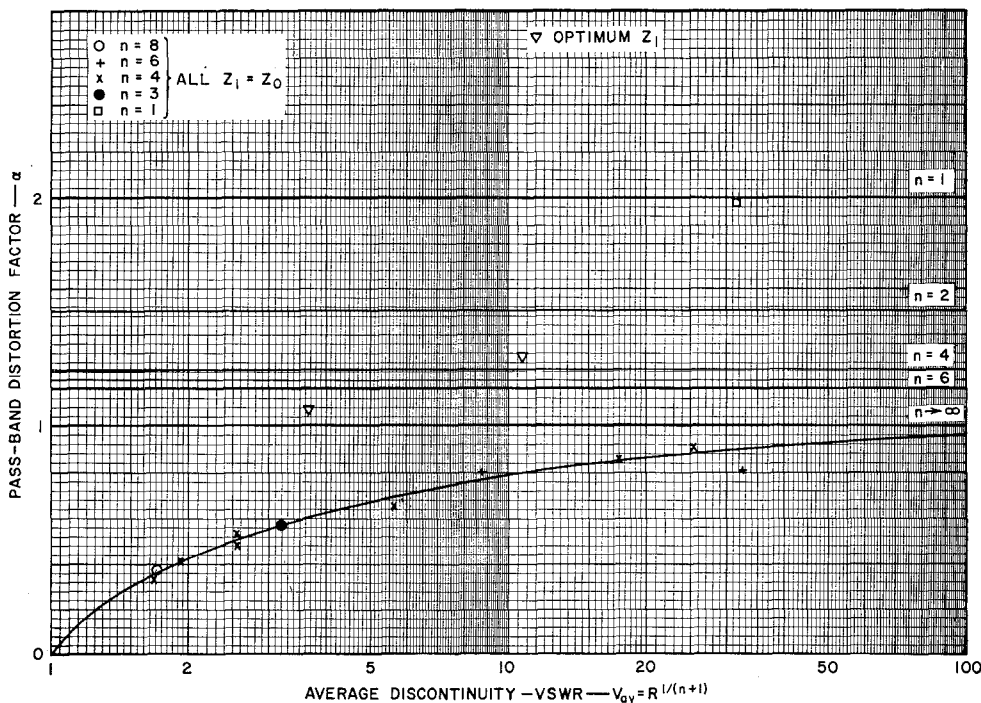


Fig. 14—Pass-band distortion factor,  $\alpha$ , vs average discontinuity VSWR,  $V_{av}$ , showing the solutions for fourteen particular cases joined by a smooth curve.

The parameter  $\alpha$  was thus calculated for fourteen widely different filters, whose response curves had been computed, having from  $n=3$  to 8 resonators plus one with  $n=1$  resonator, and for bandwidths varying from narrow (10 per cent) through medium to wide (85 per cent). These fourteen points are plotted in Fig. 14 against the average discontinuity VSWR,

$$V_{av} = R^{1/(n+1)}. \quad (26)$$

It is seen that eleven points can be joined by a smooth curve running through or very close to them. The three exceptions are explained as follows: One is for  $n=1$  (see Section VII), and then by (23) one would expect  $\alpha=2$ , which is indeed the case. The other two points, shown by triangles, correspond to nonuniform-impedance filters, to be dealt with in Section VIII. It may be concluded that the curve in Fig. 14 can generally be used to obtain the pass-band distortion factor  $\alpha$  for filters with uniform line impedances (all  $Z_i$  equal to  $Z_0$  in Figs. 1 and 2), and having more than about  $n=3$  resonators.

It can be shown from (24) and (25) that the frequency displacement  $f_m - f_0$  is given by

$$\delta = \frac{f_m - f_0}{f_m} = \frac{\Delta f_2 - \Delta f_1}{2f_m} = \left( \frac{A - 1}{A + 1} \right) \frac{w}{2} \quad (27)$$

where

$$\left. \begin{aligned} \log A &= \log (\Delta f_2 / \Delta f_1) \\ &= \alpha \log (f_2 / f_1) \\ &= \alpha \log \left( \frac{2 + w}{2 - w} \right) \end{aligned} \right\}$$

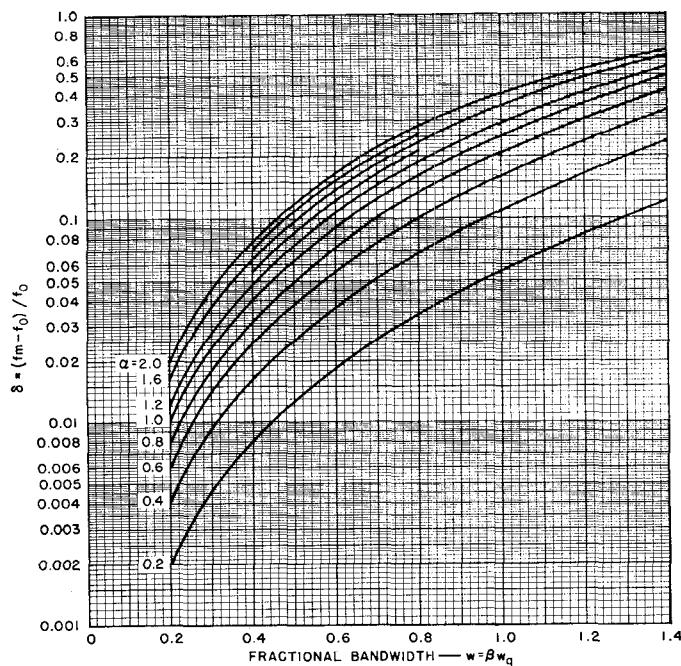


Fig. 15—Relative displacement of mean frequency from synchronous frequency,  $\delta$  as a function of fractional bandwidth for several values of  $\alpha$ .

This equation is *exact* when (24) is regarded as a definition as it is here. Eq. (27) is plotted in Fig. 15, showing the relative mean-to-synchronous frequency displacement,  $(f_m - f_0)/f_m$  as a function of the fractional bandwidth,  $w$ , for several values of the parameter  $\alpha$ . [When  $\alpha=0$ , the displacement  $(f_m - f_0)$  is zero.]

This completes the discussion of the effect on the pass-band edges of changing the discontinuities from impedance steps to reactive elements. We shall now show how the stop-band attenuation is affected by this change.

### C. Stop-Band Attenuation

A simple procedure will be developed for predicting the skirt of the filter response. The approximations made are such that this prediction holds closely over most of the rising portion of the skirt, but will be relatively less accurate very close to the band edge, as well as past the first attenuation maximum above the pass band; these are not serious limitations in practice. (The accuracy obtainable will be illustrated by several examples in Sections VI and VIII.)

The excess loss [1],  $\epsilon$ , of a stepped-impedance half-wave filter is

$$\epsilon = \frac{P_{available}}{P_{load}} - 1 = \frac{(R - 1)^2 T_n^2(\sin \theta / \mu_0)}{4R T_n^2(1/\mu_0)}, \quad (28)$$

where  $R$  is the product of the discontinuity VSWR's,

$$R = V_1 V_2 V_3 \cdots V_{n+1}. \quad (29)$$

Here,  $T_n$  is a Chebyshev polynomial of order  $n$ , and  $\mu_0$  is a constant [1]

$$\mu_0 = \sin \left( \frac{\pi w_q}{4} \right). \quad (30)$$

The response of the reactive-element filter is also given by (28) except that  $R$  is no longer constant, since the  $V_i$  become functions of frequency as a result of the changing susceptances or reactances. Therefore, at any frequency  $f$  (and for the shunt-susceptance filter of Fig. 2)

$$V_i(f) = \frac{[4 + (B_i/Y_0)^2(f_0/f)^2]^{1/2} + (B_i/Y_0)(f_0/f)}{[4 + (B_i/Y_0)^2(f_0/f)^2]^{1/2} - (B_i/Y_0)(f_0/f)} \quad (31)$$

when all the line impedances are equal. [For the series-reactance filter of Fig. 1, substitute  $(X_i/Z_0)$  for  $(B_i/Y_0)$ .] For large enough  $V_i$  and  $B_i$ , (31) reduces approximately to

$$V_i(f) \approx (B_i f_0 / f)^2. \quad (32)$$

This equation is accurate to within 20 per cent for  $|B| > 3$ , 8 per cent for  $|B| > 5$ , 2 per cent for  $|B| > 7$ , and 1 per cent for  $|B| > 8$ . For smaller  $|B|$ , (31) should be used. The numerical solution of (31) for  $f=f_0$  is the curve marked  $h=1$  in Fig. 8.

The attenuation of the filter on both skirts of the response curve may be estimated simply and fairly accurately from the known attenuation of the transformer prototype. Using (32),  $R$  becomes a function of frequency such that approximately

$$R \propto (f_0/f)^{2(n+1)}, \quad (33)$$

and by (28) the attenuation will be multiplied by the same factor when  $R$  is large. [More accurately (31) rather than (32) should be used when some of the  $V_i$  are small.] Thus to estimate the filter attenuation at a specified frequency not too close to the band edge, we may first find the transformer attenuation in decibels at the corresponding frequency and then add  $20(n+1) \log_{10}(f_0/f)$  db, as already stated in (13).

By the *corresponding frequency*, we here mean that frequency on the quarter-wave transformer characteristic,  $f'$  (Fig. 11), which is obtained from a linear scaling

$$\frac{f'}{f_1'} = \frac{f}{f_1} \quad (34)$$

or

$$\frac{f'}{f_2'} = \frac{f}{f_2}, \quad (35)$$

depending on whether the frequency  $f$  is below the lower band edge,  $f_1$ , or above the upper band edge,  $f_2$  (Fig. 11).

The stop-band attenuation of the filter can thus be predicted fairly accurately from the prototype transformer characteristic. More often the reverse problem has to be solved. Thus the quantities specified may include the stop-band attenuation of the *filter* at some frequency, besides (for instance) the pass-band ripple and bandwidth; it is then required to find the minimum number of resonators  $n$  to meet these specifications. This problem can be solved explicitly only for the prototype circuit [1]. To find the number of resonators  $n$  for the reactively coupled half-wave filter to meet a specified pass-band ripple, bandwidth, and skirt selectivity (stop-band attenuation), requires trial solutions in which numbers are assumed for  $n$  until the filter meets the specifications. Where (33) and (13) are valid, this can be worked out quickly as illustrated in the example of Section IV. Otherwise (29) and (31) should be used; the numerical solution is facilitated by the graph in Fig. 8. Usually it is not necessary to solve for all the  $V_i$ , but to solve only for one average discontinuity VSWR,  $V_{av}$ , given by (26) which saves time in making the calculations. This method is used in the last example of Section VI.

This completes the necessary background material required for the selection of transformer prototypes which will lead to filters of specified characteristics. The design procedure will now be summarized.

#### D. Summary of Design Procedure

The design procedure to be followed then consists of the following steps:

- 1) From the filter specifications select a quarter-wave transformer prototype that may be expected to yield a filter with nearly the desired performance. (The selected transformer will have the same pass-band ripple as specified for the filter.)
- 2) Determine  $\beta$  from Fig. 12, and so estimate  $w = \beta w_q$ . If  $w$  is not as specified, repeat with another transformer with different bandwidth  $w_q$  until this specification is met.
- 3) Determine  $\alpha$  from Fig. 14, and then  $\delta = (f_m - f_0)/f_m$  from Fig. 15. If  $(f_m - f_0)$  is small enough to be neglected (as will generally be the case for filters below about 10 per cent bandwidth), omit Steps 4) and 5).
- 4) If  $(f_m - f_0)$  is significant, find  $f_0$  from

$$f_0 = (1 - \delta)f_m. \quad (36)$$

This is the synchronous frequency, which is also the center frequency of the transformer.

- 5) The upper and lower band-edges,  $f_2$  and  $f_1$ , are next found from

$$\left. \begin{aligned} f_2 &= f_m \left(1 + \frac{w}{2}\right) \\ &= f_0 \left(\frac{1 + w/2}{1 - \delta}\right) \\ \text{and} \\ f_1 &= f_m \left(1 - \frac{w}{2}\right) \\ &= f_0 \left(\frac{1 - w/2}{1 - \delta}\right) \end{aligned} \right\} \quad (37)$$

- 6) The values of the reactances or susceptances and their spacings are given by (3)–(11), and must be determined at the synchronous frequency  $f_0$ .

## VI. EXAMPLES OF FILTERS HAVING MEDIUM AND LARGE BANDWIDTHS

In this section, two further examples will be given, illustrating the design of a medium-bandwidth (20 per cent), and a large-bandwidth (85 per cent) filter (all of the type shown in Figs. 1 and 2). Their predicted and analyzed performances will be compared to show how accurate the method may be expected to be.

### A. A 20 Per Cent Bandwidth Filter

It is required to design a filter with four resonators to have a pass-band VSWR of better than 1.10 over a 20 per cent bandwidth.

Thus  $n = 4$ ,  $w = 0.20$ ,  $V_r = 1.10$ .

Here  $V_r = 1.10$  is less than  $1 + (2w)^2 = 1.16$ , but not very much less; reference to Section I suggests that this is a borderline case for which the low-pass prototype will not work too well, but is worth trying. Using (12) and (6), one obtains

$$\left. \begin{aligned} \frac{B_1}{Y_0} = \frac{B_5}{Y_0} &= -0.842 \\ \frac{B_2}{Y_0} = \frac{B_4}{Y_0} &= -2.607 \\ \frac{B_3}{Y_0} &= -3.758 \end{aligned} \right\} \quad (38)$$

with

$$\left. \begin{aligned} \theta_1 = \theta_4 &= 127.67^\circ \\ \theta_2 = \theta_3 &= 147.24^\circ \end{aligned} \right\}, \quad (39)$$

which also corresponds to a quarter-wave transformer or half-wave filter that would have

$$\left. \begin{aligned} V_1 = V_5 &= 2.27 \\ V_2 = V_4 &= 8.67 \\ V_3 &= 16.07 \end{aligned} \right\}. \quad (40)$$

The product  $R = V_1 V_2 \cdots V_5$  is equal to 6215 which is only about ten times  $(1/w)^n = (1/0.2)^4 = 625$ , which confirms that this is a borderline case. [See (2).]

The analyzed performance curves of the filter defined by (38) and (39), and the stepped-impedance half-wave filter defined by (40), are plotted in Fig. 16. Neither characteristic meets the specifications very closely because the narrow-band condition, (2), is not satisfied well enough.

Let us redesign the prototype quarter-wave transformer, or stepped-impedance half-wave filter, and derive the reactance-coupled filter from the quarter-wave transformer prototype. Selecting  $n = 4$ ,  $w_q = 0.40$ ,  $V_r = 1.10$ , which by Table I of Young [1] gives  $R = 5625$ , yields

$$\left. \begin{aligned} V_1 = V_5 &= 2.398 \\ V_2 = V_4 &= 8.45 \\ V_3 &= 13.71 \end{aligned} \right\}. \quad (41)$$

These VSWR's do not seem to differ greatly from those in (40), yet they will be enough to turn the broken-line characteristic in Fig. 16 into an equi-ripple prototype response and greatly improved filter response.

From Fig. 12, for  $n = 4$  and  $R = 5625$ , one obtains  $\beta = 0.52$ , so that we would expect the reactance-coupled filter bandwidth to be  $w = \beta w_q = 0.52 \times 0.40 = 0.208$ . From Fig. 14, for

$$V_{av} = R^{(1/n+1)} = (5625)^{1/5} = 5.65, \quad (42)$$

we read off  $\alpha = 0.65$ . Hence, from Fig. 15,  $\delta = 0.0064$ .

Then, from (37)

$$\left. \begin{aligned} f_2 &= 1.110f_0 \\ f_1 &= 0.902f_0 \end{aligned} \right\} \quad (43)$$

where  $f_0$  is the synchronous frequency.

For the reactance-coupled filter derived from (41) using (6) and (11) (which assume that  $h_i = 1$ ),

$$\left. \begin{aligned} \frac{B_1}{Y_0} = \frac{B_5}{Y_0} &= -0.902 \\ \frac{B_2}{Y_0} = \frac{B_4}{Y_0} &= -2.563 \\ \frac{B_3}{Y_0} &= -3.436 \end{aligned} \right\}, \quad (44)$$

and therefore

$$\left. \begin{aligned} \theta_1 = \theta_4 &= 128.15^\circ \\ \theta_2 = \theta_3 &= 145.92^\circ \end{aligned} \right\}. \quad (45)$$

The analyzed response of the stepped-impedance half-wave filter prototype corresponding to the exact Chebyshev transformer design (41) is shown by the broken line in Fig. 17, and the reactance-coupled filter

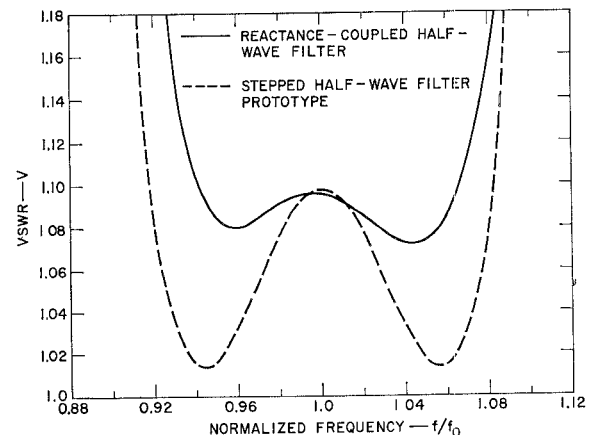


Fig. 16—Characteristics of a four-resonator filter and its stepped half-wave filter prototype, both based on an equal-ripple low-pass, lumped-constant prototype.

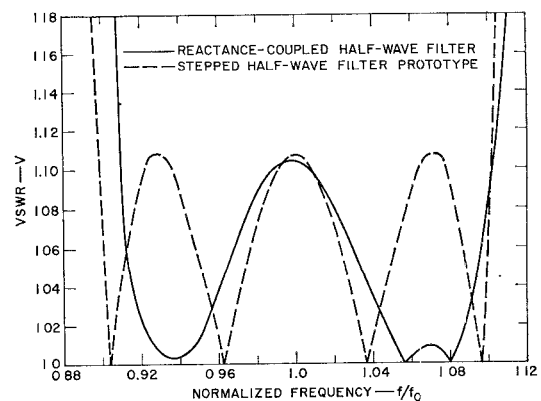


Fig. 17—Characteristics of a four-resonator filter and its equal-ripple stepped half-wave filter prototype.

response is shown by the solid line in that figure. This is an appreciable improvement on the performance of the preceding filter and transformer design based on the first procedure using the lumped-constant low-pass prototype. The analyzed performance of the filter shows that  $f_1=0.909f_0$  (compare  $0.902f_0$  predicted) and  $f_2=1.103f_0$  (compare  $1.110f_0$  predicted). The fractional bandwidth  $w$  is 0.193 (compare 0.208 predicted), and the relative mean-to-synchronous frequency displacement  $\delta=(f_m-f_0)/f_m$  is 0.006 (just as predicted).

It is clear, comparing the solid and broken lines of Fig. 17, that there is still room for improvement. The main discrepancy between predicted and analyzed performance is in the bandwidth, which is 1.5 per cent less than predicted. The reason for this is the difference in the frequency sensitivities of the resonator lengths; this difference is typical of filters in which some of the discontinuity VSWR's are in the neighborhood of 2.0, and others differ appreciably from the value 2.0 [see (41)]. The reason for this will be explained in Section VII. This example will then be continued in the first example of Section VIII where it will be shown that the line-length frequency sensitivities can be equalized by optimizing the line impedances (instead of setting them all equal to each other). This generally leads to a very nearly equal-ripple characteristic with slightly more than the predicted bandwidth.

### B. An 85 Per Cent Bandwidth Filter

A pseudo-high-pass filter of eight sections is to be designed to have a pass-band frequency ratio  $f_2/f_1$  of approximately 2.5:1, and a pass-band attenuation (reflection-loss) of less than 0.1 db.

Since  $f_2/f_1=2.5$ ,

$$w = 2 \left( \frac{f_2 - f_1}{f_2 + f_1} \right) \approx 0.85. \quad (46)$$

We design a quarter-wave transformer prototype by the modified first-order theory [1], specifying  $w_q=1.40$ , and a 0.2-dB pass-band attenuation ripple. (This approximate method always gives slightly less bandwidth, and slightly less ripple, than specified.) The modified first-order theory gives

$$\left. \begin{aligned} V_1 &= V_9 = 1.348 \\ V_2 &= V_8 = 1.561 \\ V_3 &= V_7 = 1.829 \\ V_4 &= V_6 = 1.985 \\ V_5 &= 2.034 \end{aligned} \right\}. \quad (47)$$

The computed response is shown by the broken line in Fig. 18, and it is seen that it has a pass-band attenuation of less than 0.12 db over a 135 per cent bandwidth ( $w_q=1.35$ ). The quarter-wave transformer output-to-input impedance ratio  $R$  is

$$R = V_1 V_2 \cdots V_9 = 118.4. \quad (48)$$

From Fig. 12, the bandwidth contraction factor is  $\beta=0.63$ , and the expected fractional bandwidth of the filter is therefore  $w=\beta w_q=0.85$ , which is the specified bandwidth.

We also find from Fig. 14 that for  $V_{av}=(118.4)^{1/9}=1.70$ ,  $\alpha=0.36$ . Then, from Fig. 15, one obtains  $\delta=0.06$ .

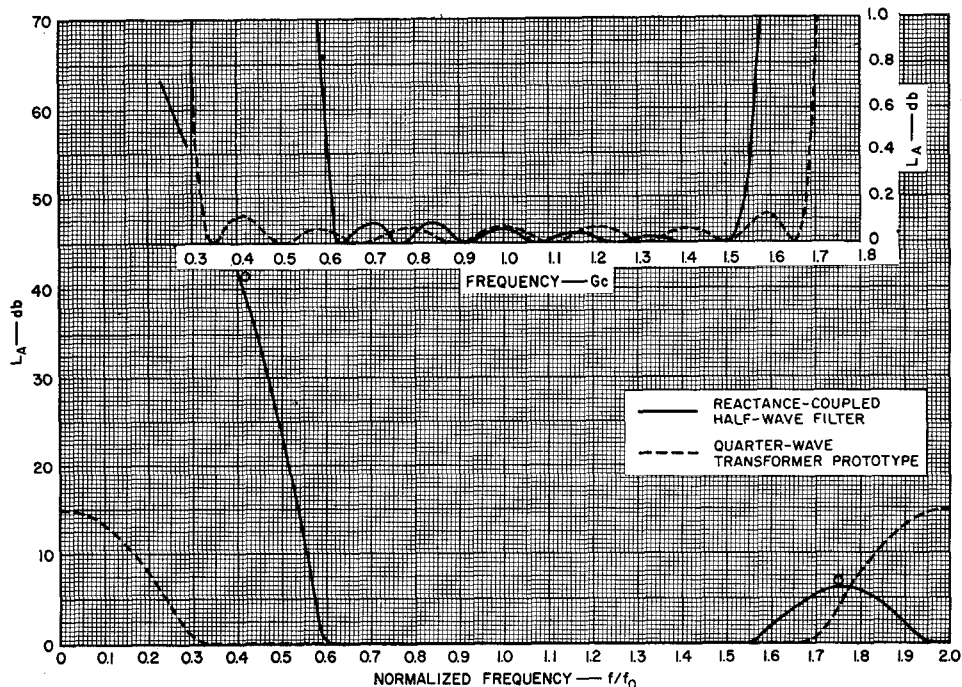


Fig. 18—Characteristics of an eight-resonator filter and its quarter-wave transformer prototype.

Therefore, by (37), we shall expect

$$\left. \begin{aligned} f_2 &= 1.52f_0 \\ f_1 &= 0.61f_0 \end{aligned} \right\} \quad (49)$$

For the reactance-coupled filter derived from (47) by use of the equations in Section III with  $h_i=1$ ,

$$\left. \begin{aligned} \frac{B_1}{Y_0} = \frac{B_9}{Y_0} &= -0.2998 \\ \frac{B_2}{Y_0} = \frac{B_8}{Y_0} &= -0.4495 \\ \frac{B_3}{Y_0} = \frac{B_7}{Y_0} &= -0.613 \\ \frac{B_4}{Y_0} = \frac{B_6}{Y_0} &= -0.700 \\ \frac{B_5}{Y_0} &= -0.725 \end{aligned} \right\}, \quad (50)$$

and

$$\left. \begin{aligned} \theta_1 = \theta_8 &= 100.60^\circ \\ \theta_2 = \theta_7 &= 104.85^\circ \\ \theta_3 = \theta_6 &= 108.17^\circ \\ \theta_4 = \theta_5 &= 109.61^\circ \end{aligned} \right\} \quad (51)$$

The response of this filter was analyzed and is shown by the solid line in Fig. 18. It is seen that the attenuation in the pass band is everywhere less than 0.1 db, the fractional bandwidth  $w$  is 0.85, the band edges are  $f_2=1.53$  and  $f_1=0.62$ , and the relative mean-to-synchronous frequency displacement is 0.075; all of these are very close to the predicted values.

The stop-band attenuation was worked out at two frequencies, as explained in Section V. [Fig. 8, based on (31), was utilized in this calculation.] These two points are shown by the small rings in Fig. 18, and fall very close to the curve obtained by analysis on a digital computer.

It is possible to increase the selectivity of a filter by adding more resonators. Good results have been obtained by taking a design with fewer resonator-cavities than necessary to obtain the required stop-band attenuation, and then adding more cavities by repeating the middle cavity as often as necessary. For instance, the design given in (50) and (51) was modified as follows: The central elements, which are nearly the same (0.700, 0.725, 0.700), were set equal to their average value (0.71). More elements with this value were added, spaced for synchronous tuning, as in (11), and the response computed up to 15 resonators [9]. It was found that the pass-band ripple amplitude and bandwidth changed very little, while the skirt selectivity increased with each added cavity.

## VII. DERIVATION OF THE DATA FOR BANDWIDTH CONTRACTION AND PASS-BAND DISTORTION

The basic ideas on the conversion of the quarter-wave transformer prototype into a filter with reactive elements have already been explained. The design procedure and numerical data were presented, mostly without proof. We now proceed to fill in the details of the over-all picture present thus far.

### A. Bandwidth Contraction

The frequency sensitivity [1], [2] (and hence bandwidth) of the reactance-coupled filters of Figs. 1 and 2 is strongly influenced by the angles  $\psi'$  and  $\psi''$  in Fig. 9, which correspond to the electrical distances between the coupling reactance and the two reference planes with pure imaginary reflection coefficient on either side of it. Both reference planes move closer to the reactance as the frequency increases, partly 1) because a given *electrical* separation shrinks in *physical* length as the frequency increases; and partly 2) because the *electrical* lengths  $\psi'$  and  $\psi''$  do not remain constant, but decrease with increasing frequency for shunt inductances (or series capacitances), since their susceptance (or reactance) values decrease with frequency. The movement of the reference planes is measured quantitatively by two parameters  $d'$  and  $d''$  defined by

$$d' = \frac{4}{\pi} \left[ \psi' - \frac{d\psi'}{d(f/f_0)} \right]_{f=f_0} \quad (52)$$

$$d'' = \frac{4}{\pi} \left[ \psi'' - \frac{d\psi''}{d(f/f_0)} \right]_{f=f_0}, \quad (53)$$

where the first term in the square brackets corresponds to Cause 1), and the second term to Cause 2). The parameters  $d'$  and  $d''$  measure the rate of change with frequency of the reference planes in Fig. 9, as compared to the rate of change of a  $45^\circ$  line length. The spacings  $\theta_i$  (Figs. 1 and 2) between reactances are given at band center by (9). The spacings are thus always longer electrically than  $90^\circ$ , and accordingly increase with frequency faster than does a quarter-wave length of line. The bandwidth of the filter is thus always less than the bandwidth of its quarter-wave transformer prototype by a factor  $\beta$ . The bandwidth contraction factor associated with the  $i$ th resonator or line section  $\beta_i$ , is given by

$$\frac{1}{\beta_i} = \frac{2}{\pi} \left[ \frac{d\theta_i}{d(f/f_0)} \right]_{f=f_0} = 1 + \frac{d_i'' + d_{i+1}'}{2}. \quad (54)$$

If all the  $\beta_i$ , defined in (54) were the same for a particular filter, then its bandwidth would be

$$w = \beta w_q, \quad (55)$$

where  $w_q$  is the quarter-wave transformer bandwidth. Usually the  $\beta_i$  are not all equal; the smallest of the  $\beta_i$  should then be used for  $\beta$  in the above equation since the most frequency-sensitive resonator tends to determine the filter bandwidth.

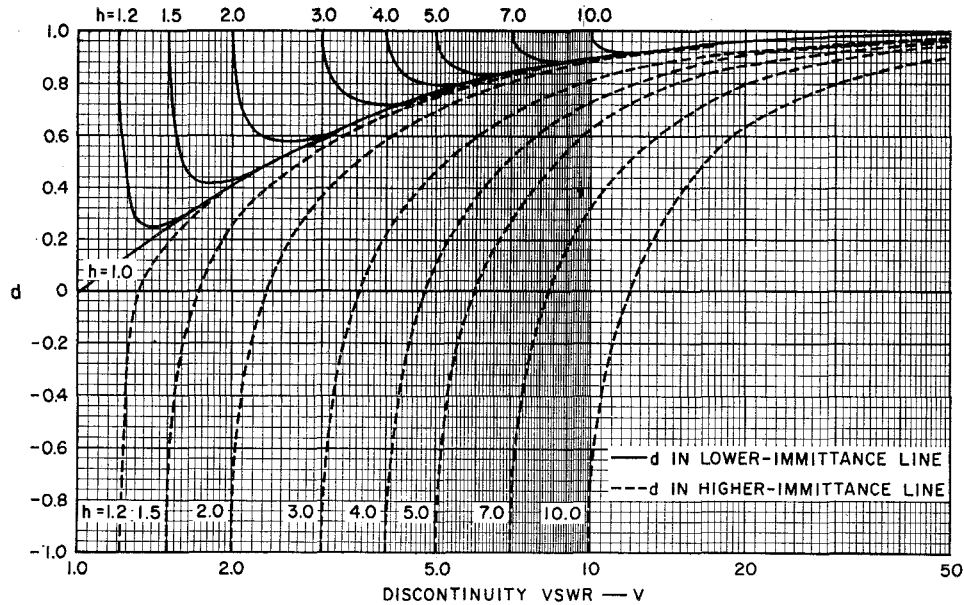


Fig. 19—Chart determining frequency sensitivities of individual resonators over small frequency bands.

To cover both the series-reactance-coupled and the shunt-susceptance-coupled filter in Figs. 1 and 2, we shall use the word immittance when we mean impedance for the former (Fig. 1) or admittance for the latter (Fig. 2). When the line immittances are all equal, then  $d_i' = d_i''$ , but when the line immittances are not all equal, the  $d_i'$  and  $d_i''$  are not equal. The larger  $d_i$  is associated with the  $\psi_i$  in the line with lower immittance, and is given by the solid lines in Fig. 19; conversely, the smaller  $d_i$  is associated with the  $\psi_i$  in the line with higher immittance, and is given by the broken lines in Fig. 19. The curves in Fig. 19 were worked out for infinitesimal bandwidths, following (52) and (53). The curves in Fig. 20 were worked out for several finite bandwidths, replacing the differential terms in (52) and (53) by finite increment ratios. Only filters with uniform line immittances ( $h_i = 1$ ) are shown in Fig. 20. Fig. 12 was then worked out with the aid of the curve  $h = 1$  in Fig. 19, which is the same as the curve  $w = 0$  in Fig. 20.

It has been found that Fig. 12 has predicted bandwidths closely for all the filters analyzed. The accuracy is least for filters that have a considerable spread among their  $\beta_i$ . According to (54) and Figs. 19 or 20, this occurs when the discontinuity VSWR's in one filter range into and out of the neighborhood of 2.0, where  $d$  can change appreciably in either direction (see Figs. 19 or 20). In that case it may be worthwhile to optimize the line impedances, as in Section VIII.

### B. Pass-Band Distortion

The distinction has already been made between the synchronous frequency  $f_0$  and the arithmetic mean frequency  $f_m$ , which is always greater than  $f_0$ , since the portion of the pass band above the synchronous frequency is greater than the portion below. This phenomenon is due to the declining discontinuity VSWR's with increas-

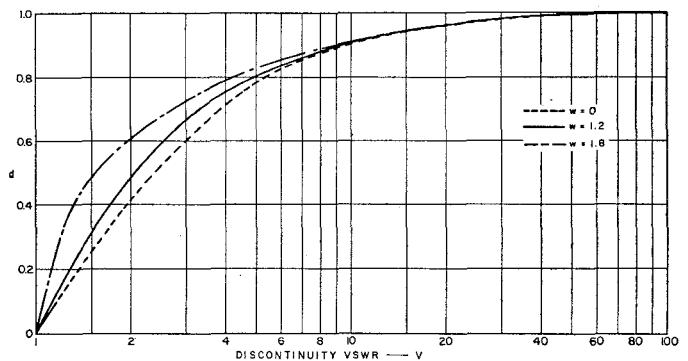


Fig. 20—Chart determining frequency sensitivities of individual resonators over various fractional bandwidths,  $w$ , when the line impedances are constant.

ing frequency when series capacitances or shunt inductances are used, and may be put on a quantitative footing as follows.

The excess loss has already been cited in (28). Consider now the case of large  $R$ , so that the approximation (32) holds. The largest term of the Chebyshev polynomial well inside the stop band is the highest power of  $(\sin \theta/\mu_0)$ , and then (28) reduces to

$$\varepsilon = \frac{P_{\text{avail}}}{P_{\text{load}}} - 1 \approx \text{const.} \frac{\sin^{2n} \theta}{(f/f_0)^{2(n+1)}} \quad (56)$$

$$\approx \text{const.} \left[ \frac{\Delta f}{(f/f_0)^{1+1/n}} \right]^{2n}, \quad (57)$$

where  $\Delta f = f - f_0$ . This proves the result stated in (22) and (23); for large  $n$  and large  $R$ , the exponent of  $(f/f_0)$  reduces to unity, leading to a more symmetrical response on a wavelength (rather than frequency) scale. As a counter-example, a single-resonator filter ( $n=1$ ) was analyzed and  $\alpha$  calculated from (24). The response of this filter ( $n=1$ ,  $R=1000$ ) is plotted in Fig. 21, and it

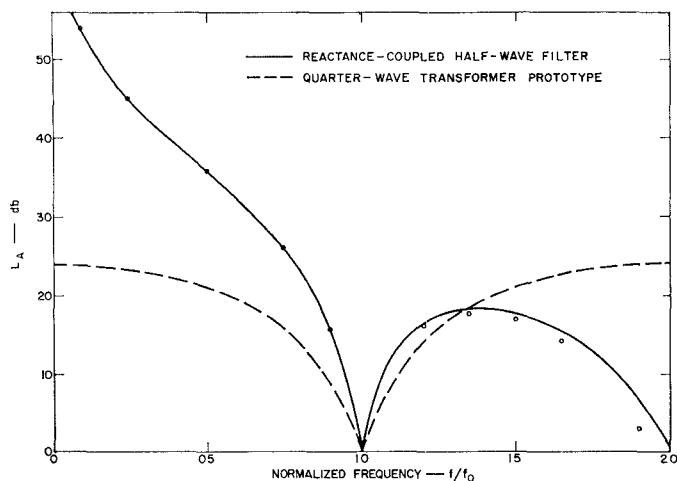


Fig. 21—Characteristics of a single-section filter and its quarter-wave transformer prototype.

was found that (using the 14-db band edges for convenience)  $\alpha = 1.97$ , which is close to  $1 + 1/n = 2.0$  as required for  $n = 1$ . This point is shown square in Fig. 14.

The circle points in Fig. 21 were calculated using the approximate (13) in conjunction with the prototype characteristic. This method is seen once again to give excellent results.

The choice of mapping or frequency distortion by a function of the form  $\Delta f/(f/f_0)^\alpha$ , was based on the above considerations, and is further developed in Section V.

### VIII. OPTIMIZING THE LINE IMPEDANCES

It was pointed out in Section VII that different line sections of a single filter yield different bandwidth contraction factors  $\beta_i$ , because the quantities  $d_i'$ ,  $d_i''$  vary from resonator to resonator. So far we have only considered examples of filters with uniform line impedances, where all  $Z_i$  are equal to  $Z_0$ . In deriving the discontinuity parameters, the discontinuity VSWR is always set equal to the corresponding step VSWR of the prototype transformer; this VSWR can be obtained in the filter by an infinity of combinations of reactances with impedance ratios since the *two* parameters  $h$  and  $u$  (Fig. 9) produce the desired discontinuity VSWR. Thus, if  $V_i$  is given and  $h_i$  is selected,  $X_i$  or  $B_i$  is determined from (4) and (5). The problem is now to select  $h_i$ ,  $V_i$  being given, so that all the  $\beta_i$  are the same. This can easily be done with the aid of Fig. 19, and is best illustrated by an example.

#### A. A 20 Per Cent Bandwidth Filter with Optimized Line Impedances

It is required to improve the performance of the filter defined by (44) and (45) and shown by the solid line in Fig. 17.

We see from (41) that the  $V_i$  range in numerical value from about 2 to nearly 14. Thus the different resonators have appreciably different  $\beta_i$ , and we might expect a noticeable deviation from an equal-ripple

response, as already pointed out for this situation.

Here we have a four-resonator filter. The two central resonators, 2 and 3, are each flanked by discontinuity VSWR's of 8.45 and 13.71, according to (41). Keeping the characteristic admittances of the lines forming the four resonators the same, we find from Fig. 19 that  $d_2'' = 0.88$  (corresponding to  $h = 1$ ,  $V = 8.45$ ) and  $d_3' = 0.93$  (corresponding to  $h = 1$ ,  $V = 13.71$ ), so that for the two central resonators,

$$\frac{d_2'' + d_3'}{2} = \frac{d_3'' + d_4'}{2} = 0.905. \quad (58)$$

If we kept the input and output admittances the same also, so that  $h = 1$  at both the first and last discontinuities, then for  $V = 2.398$ , (41), we would have  $d_1'' = 0.50$ , which is considerably different from the other  $d$ . Since  $d_2' = d_2'' = 0.88$ , this would yield  $(d_1'' + d_2')/2 = 0.69$  for the outside resonators, which differs appreciably from 0.905 for the central resonators. Hence the relatively poor response shape in Fig. 17. To obtain a value of  $(d_1'' + d_2')/2$  equal to 0.905, as for the central resonators, requires  $d_1'' = d_3' = 0.93$ . We then find the value of  $h$  from Fig. 19. Finding the intersection of the horizontal line for  $d = 0.93$  with the vertical line for  $V = 2.398$  gives  $h = 2.38$ . One then obtains the following filter parameters:

$$\frac{Y_1}{Y_0} = \frac{Y_2}{Y_0} = \frac{Y_3}{Y_0} = \frac{Y_4}{Y_0} = \frac{1}{2.38} = 0.4202 \quad (59)$$

$$\left. \begin{aligned} \frac{B_1}{Y_0} = \frac{B_5}{Y_0} &= -0.7895 \\ \frac{B_2}{Y_1} = \frac{B_4}{Y_1} &= -2.564 \\ \frac{B_3}{Y_1} &= -3.433 \end{aligned} \right\} \quad (60)$$

$$\left. \begin{aligned} \theta_1 = \theta_4 &= 158.74^\circ \\ \theta_2 = \theta_3 &= 145.92^\circ \end{aligned} \right\} \quad (61)$$

The predicted bandwidth is

$$w = \beta w_q = 0.40/1.905 = 0.210. \quad (62)$$

The appearance of such a filter with shunt-inductive irises in waveguide, or with series-capacitive gaps in strip line, is shown in Fig. 22.

The analyzed performance of this filter is shown by the solid line (marked C) in Fig. 23. The original design, obtained from a constant low-pass prototype through (12) and (6), is shown for comparison (curve A); the performance of the filter based on the same transformer prototype as curve C, but with *uniform* line impedances (all  $h_i = 1$ : see Section VI) is also shown (curve B). It is seen that the new design, after optimizing the line impedances, gives an almost equal-ripple response. Its

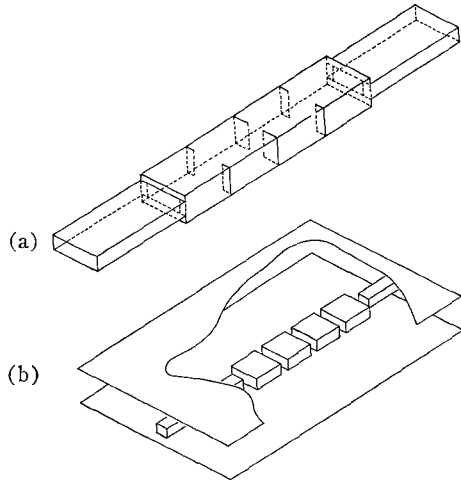


Fig. 22—Filters in which the line impedances change.

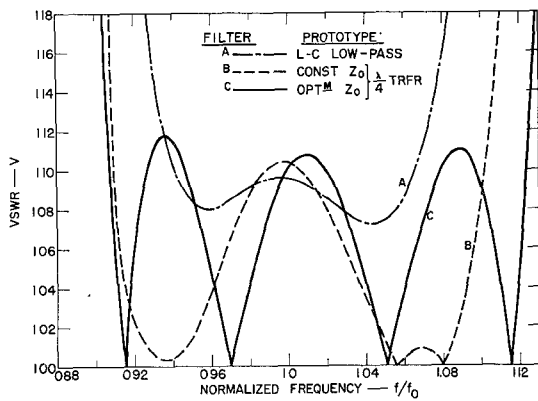


Fig. 23—Characteristics in the pass band of three filters designed to the same specifications.

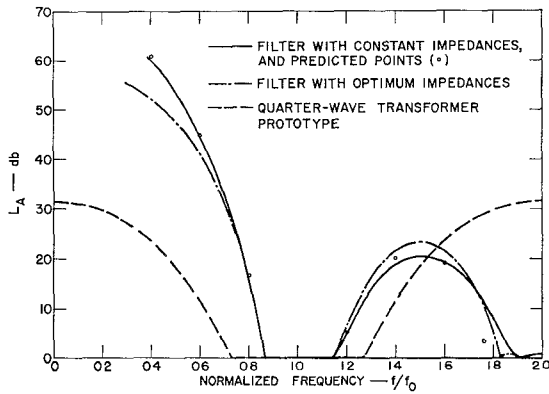


Fig. 24—Characteristics in the stop band of the three filters described in Fig. 23.

bandwidth is 21.8 per cent, slightly more than the 21.0 per cent predicted.

The distortion factor  $\alpha$  worked out from (24) amounts to 1.33, and is shown by the upper triangle point in Fig. 14. It does not fall in line with the points calculated for the constant-line-impedance filters. Most of the improvement in bandwidth is due to an increase in the upper band-edge frequency (Fig. 23) which has

the effect of increasing  $\alpha$ . A possible explanation is that  $V_1$  and  $V_5$  are largely determined by the impedance step, which is independent of frequency, whereas the other VSWR's ( $V_2$ ,  $V_3$ , and  $V_4$ ) are determined by reactances which decrease as the frequency rises. This corresponds, on the high-frequency side, to having the filter turn into a wider band design, thus pushing the upper band edge even further up. The reverse holds (the  $V_i$  increase) below band center, which here partly cancels the improvement in bandwidth due to making all  $\beta_i$  equal to one another, and so the lower band edge moves less. Thus  $\alpha$  increases by (24).

The pass- and stop-band responses of the two filters based on the same quarter-wave transformer prototype are shown in Fig. 24, along with the response of the transformer. The circle points were calculated for the uniform-line impedance filter curve (B in Figs. 23 and 24) by the method described in Section V.

b. A 30 Per Cent Bandwidth Filter

The following example is worked the same way as the previous one, and only the results are given. It is based on the following prototype Chebyshev transformer:

$$\left. \begin{aligned} n &= 4 \\ R &= 100 \\ w_q &= 0.6 \\ \text{Ripple VSWR} &= 1.07 \end{aligned} \right\} \quad (63)$$

giving

$$\left. \begin{aligned} V_1 &= V_5 = 1.538 \\ V_2 &= V_4 = 3.111 \\ V_3 &= 4.368 \end{aligned} \right\} \quad (64)$$

Transformed into a filter with uniform line impedances, the reactance parameters and line lengths are

$$\left. \begin{aligned} \frac{B_1}{Y_0} &= \frac{B_5}{Y_0} = -0.4335 \\ \frac{B_2}{Y_0} &= \frac{B_4}{Y_0} = -1.1971 \\ \frac{B_3}{Y_0} &= -1.6115 \end{aligned} \right\} \quad (65)$$

$$\left. \begin{aligned} \theta_1 &= \theta_4 = 111.57^\circ \\ \theta_2 &= \theta_3 = 124.88^\circ \end{aligned} \right\} \quad (66)$$

This example has been selected because of the appreciable spread of  $V_i$  about the numerical value 2.

With these values of  $V_i$  and all  $Z_i = Z_0$ , Fig. 19 shows a considerable variation in  $d$  from about 0.25 to 0.75, and we would expect these different frequency sensitivities to result in a poor response shape. This is borne

out in Fig. 25, in which curve A is the filter response analyzed on a digital computer. It has a bandwidth of 30.7 per cent, compared to 34.7 per cent predicted.

To optimize the line impedances, Fig. 19 determines  $h = 1.5$  for the end couplings, and one obtains

$$\frac{Y_1}{Y_0} = \frac{Y_2}{Y_0} = \frac{Y_3}{Y_0} = \frac{Y_4}{Y_0} = \frac{1}{1.5} = 0.6667 \quad (67)$$

$$\left. \begin{aligned} \frac{B_1}{Y_0} &= \frac{B_5}{Y_0} = -0.1198 \\ \frac{B_2}{Y_1} &= \frac{B_4}{Y_1} = -1.1971 \\ \frac{B_3}{Y_1} &= -1.6115 \end{aligned} \right\} \quad (68)$$

$$\left. \begin{aligned} \theta_1 &= \theta_4 = 142.62^\circ \\ \theta_2 &= \theta_3 = 124.88^\circ \end{aligned} \right\} \quad (69)$$

The physical appearance of this filter would again be as indicated in Fig. 22. The response of the filter was analyzed and is plotted as curve B in Fig. 25. Again there is very nearly an equal-ripple response, and the bandwidth is 36.2 per cent, which is slightly more than the 35.8 per cent predicted. Most of the improvement in bandwidth occurs above the band center. A possible explanation for this effect was offered in the previous example. The distortion factor  $\alpha$  here equals 1.07 and is shown by the lower triangle point in Fig. 14.

Most of the end-coupling VSWR of 1.538 is due to the impedance ratio of 1.50, and only a small part is due to the normalized susceptance of 0.1198. Since most of  $V_1 = V_5 = 1.538$  is due to the 1.5:1 impedance step, it is of practical interest to investigate what happens to the performance when the reactances  $B_1$  and  $B_5$  are left out, and the impedance ratio is increased to 1.538:1 to achieve the desired  $V_1$  and  $V_5$ . The result is

$$\frac{Y_1}{Y_0} = \frac{Y_2}{Y_0} = \frac{Y_3}{Y_0} = \frac{Y_4}{Y_0} = \frac{1}{1.538} = 0.6502 \quad (70)$$

$$\left. \begin{aligned} \frac{B_1}{Y_0} &= \frac{B_5}{Y_0} = 0 \\ \frac{B_2}{Y_1} &= \frac{B_4}{Y_1} = -1.1971 \\ \frac{B_3}{Y_1} &= -1.6115 \end{aligned} \right\} \quad (71)$$

$$\left. \begin{aligned} \theta_1 &= \theta_4 = 150.45^\circ \\ \theta_2 &= \theta_3 = 124.88^\circ \end{aligned} \right\} \quad (72)$$

The analyzed performance of this filter is shown in Fig. 25 by curve C. This filter has passed beyond the optimum performance; the peak reflection has almost doubled in the pass band, and the ripples are no longer equal. Even so, this performance is better than the first design with uniform line impedances (curve A).

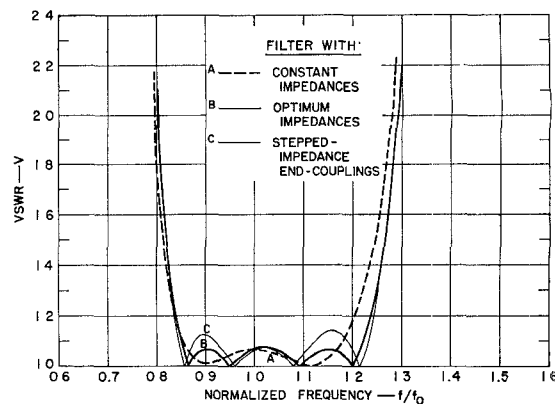


Fig. 25—Pass-band characteristics of three filters designed for 30 per cent bandwidth.

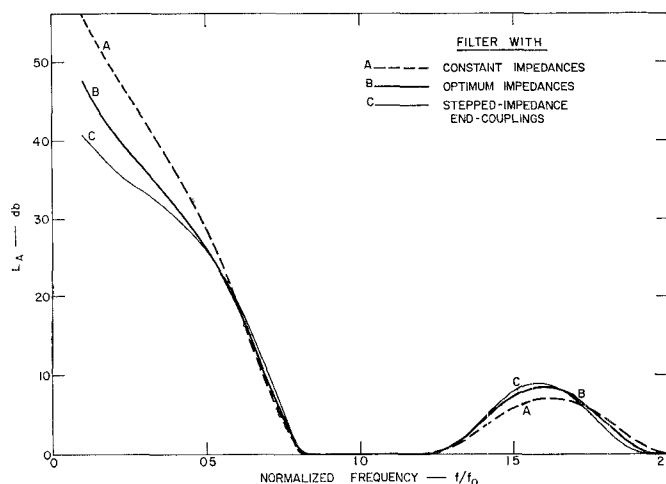


Fig. 26—Stop-band characteristics of three filters designed for 30 per cent bandwidth.

The pass-band and stop-band characteristics of all three filters are shown in Fig. 26, and are in the expected relationships to each other, since the end couplings of design A have the most capacitance, and those of design C have none.

## IX. CONCLUSION

Design procedures for reactance-coupled half-wave filters have been given, based on quarter-wave transformer prototype circuits. Each filter has the same number of discontinuities as its step-transformer prototype with corresponding discontinuities of the filter and step transformer having the same VSWR. Both the filter and its prototype were synchronously tuned circuits, which means that adjacent discontinuities had out-of-phase reflection coefficients giving the maximum cancellation. This condition determines the spacing between discontinuities. It was also shown how the line impedances of a reactance-coupled filter may be chosen to obtain a nearly equal-ripple response.

Design data and graphs were given to facilitate the prediction of filter performance when the filter is based on a selected prototype transformer. The method of

design is to first select a prototype transformer and then to see if the predicted filter performance matches the specifications. If necessary, another prototype transformer has to be selected to yield another filter meeting the specifications more closely. This was illustrated by several numerical examples having fractional bandwidths from 10 to 85 per cent.

#### ACKNOWLEDGMENT

The author is grateful to Dr. G. L. Matthaei for reading the manuscript and making many helpful suggestions, and to W. P. Datillo of the U. S. Army Research and Development Laboratory for his interest in this work and for proofreading the manuscript.

The calculations on the Burroughs Datatron 220 were programmed by P. H. Omlor.

#### REFERENCES

- [1] L. Young, "Stepped-impedance transformers and filter prototypes," *IRE TRANS. ON MICROWAVE THEORY AND TECHNIQUES*, vol. MTT-10, pp. 339-359; September, 1962.
- [2] —, "The quarter-wave transformer prototype circuit," *IRE TRANS. ON MICROWAVE THEORY AND TECHNIQUES*, vol. MTT-8, pp. 483-489; September, 1960.
- [3] G. L. Matthaei, "Design of wide-band (and narrow-band) band-pass microwave filters on the insertion loss basis," *IRE TRANS. ON MICROWAVE THEORY AND TECHNIQUES*, vol. MTT-8, pp. 580-593; November, 1960.
- [4] S. B. Cohn, "Direct-coupled-resonator filters," *PROC. IRE*, vol. 45, pp. 187-196; February, 1957. See also, J. Reed and S. B. Cohn, *PROC. IRE (Correspondence)*, p. 880, June 1957, for a discussion on the frequency dependence of the coupling elements.
- [5] H. J. Riblet, "A unified discussion of high-Q waveguide filter design theory," *IRE TRANS. ON MICROWAVE THEORY AND TECHNIQUES*, vol. MTT-6, pp. 359-368; October, 1958.
- [6] L. Young, "Twenty useful Smith chart formulas," *Microwaves*, vol. 1, pp. 30-35; June, 1962.
- [7] G. L. Matthaei *et al.*, "Design criteria for Microwave Filters and Coupling Structures," Stanford Research Inst., Menlo Park, Calif., Final Report, SRI Project 2326, Contract No. DA 36-039 SC-74862, Tables, pp. 202-203; January, 1961. Also, Tech. Note 4 on same project, Tables, pp. 19-20.
- [8] L. Young, "Peak internal fields in direct-coupled-cavity filters," *IRE TRANS. ON MICROWAVE THEORY AND TECHNIQUES*, vol. MTT-8, pp. 612-616; November, 1960.
- [9] L. Young and B. M. Schiffman, "A useful high-pass filter design," *The Microwave J.*, vol. 6, pp. 78-80; February, 1963.

#### On shunt-inductive couplings in waveguide:

- [10] N. Marcuvitz, "Waveguide Handbook," *M.I.T. Rad. Lab. Ser.* McGraw-Hill Book Co., Inc., New York, N. Y.; vol. 10, pp. 221-228; 1951.

- [11] H. Gruenberg, "Symmetrically placed inductive posts in rectangular waveguide," *Canad. J. Phys.* vol. 30, pp. 211-217; 1952.
- [12] G. Craven and L. Lewin, "Design of microwave filters with quarter-wave couplings," *Proc. IEE (London)*, vol. 103B, pp. 173-177; March, 1956.
- [13] J. C. Simon and G. Broussaud, "Les Filtres Passe-Bande en hyperfréquence," *Ann. Radioélectricité*, vol. 3, pp. 3-19; 1953.
- [14] L. Lewin, "Advanced Theory of Waveguides," Iliffe and Sons, Ltd., London, England, 1951.
- [15] J. Schwinger, Lecture Notes, prepared by David S. Saxon, Research Lab. of Electronics, Mass. Inst. Tech., Cambridge; February, 1945.
- [16] T. Moreno, "Microwave Transmission Design Data," Dover Publications, Inc., New York, N. Y.; 1948.

#### On shunt-inductive couplings in coaxial line:

- [17] C. E. Muehe, "The Inductive Susceptance of Round Metal Posts Mounted in Coaxial Line," M.I.T. Lincoln Lab., Lexington, Mass., Group Rept. 46-32; November 5, 1958.
- [18] H. Smith, "Design of symmetrical bandpass filters," *Electronic Design (Microwaves Section)*, vol. 10, pp. 40-43; April 12, 1962. (Note: These data apply only to 50-ohm line.)

#### On series-capacitance couplings in coaxial line:

- [19] L. Young, "The practical realization of series-capacitive couplings for microwave filters," *The Microwave J.*, vol. 5, pp. 79-81; December, 1962.
- [20] W. J. Getsinger, "Coupled rectangular bars between parallel plates," *IRE TRANS. ON MICROWAVE AND TECHNIQUES*, vol. MTT-10, pp. 65-72; January, 1962.

#### On quarter-wave resonator filters:

- [21] G. L. Matthaei, "Direct-coupled band-pass filters with  $\lambda_0/4$  resonators," 1958 IRE NATIONAL CONVENTION RECORD, vol. 6, pt. 1, pp. 98-111.
- [22] G. L. Matthaei and L. Young, "Microwave Filters and Coupling Structures," Stanford Research Inst., Menlo Park, Calif., Quarterly Progress Rept. 5, SRI Project 3527, Contract DA 36-039 SC-87398; April, 1962.

#### Further references on band-pass filters:

- [23] G. L. Ragan, "Microwave Transmission," *M.I.T. Rqd. Lab. Ser.*, McGraw-Hill Book Co., Inc., New York, N. Y., vol. 9, pp. 540-716; 1948.
- [24] "Very High Frequency Techniques," Harvard University, Rad. Res. Lab., McGraw-Hill Book Co., Inc., New York, N. Y., vol. 2, ch. 26-27; 1947.
- [25] E. S. Hensperger, "A simplified approach to the design of band-pass filters in waveguide," *The Microwave J.*, vol. 2, pp. 39-44; November, 1959.
- [26] R. Levy, "An improved design procedure for the multi-section generalized microwave filter," *Proc. IEE (London)*, vol. 104C, pp. 423-432; September, 1957.
- [27] —, "A guide to the practical application of Chebyshev functions to the design of microwave components," *Proc. IEE (London)* vol. 106C, pp. 193-199; September, 1959.
- [28] S. S. Forte, "The design of band-pass filters in waveguides," *Marconi Rev.*, vol. 22, pp. 99-116; 2nd Quarter, 1959.